



The influence of a lunar lander on the temperature of the surrounding surface

Ramona Ziese^{1,2,3}, Jörg Knollenberg³, Maximilian Hamm^{1,3}, Matthias Grott³, and Heike Rauer^{1,3}

¹Institute of Geological Sciences, Freie Universität, Berlin, Germany (ramona.ziese@fu-berlin.de)

²Institute of Geodesy and Geoinformation Science, Technische Universität Berlin, Berlin, Germany

³Institute of Space Research, DLR, Berlin, Germany

Introduction: With the possible return of mankind to the Moon comes the need for detailed analyses of ambient conditions in possible landing regions. Several missions (e.g. IM-2, Blue Ghost M1) have already landed in the Moon's south pole region to study the environmental conditions, and more are planned. Of particular interest are temperature measurements as they can be used to draw conclusions about the material properties of the regolith such as the surface roughness or the thermal inertia. However, any lander affects the temperature of the ground around it. This effect is particularly strong in the polar regions. Here, the ground is hit by sunlight at a large angle, while for the sides of the lander the incidence angle can be very small. Consequently, a relatively large amount of light can be scattered from the lander to the ground increasing the temperature there. Furthermore, the lander may heat up more strongly, which (depending on the emissivity of the lander's surface) could lead to comparatively large thermal emissions. This study investigates the temperature change caused by a lander located at a latitude of -84.7715° and a longitude of 29.21994° , close to the landing site of Intuitive Machines' IM-2 mission.

Methods: The lander is modeled as a cube with a side length of 1m. To disentangle the influence of the lander from the influence of the local topography, the lander's neighborhood is modeled by a plane. Both the cube and the plane are modelled using triangular meshes with side lengths of 50 cm and 12.5 cm, respectively. We assume that the lander's surface is either covered by black paint (solar albedo 0.04, IR emissivity 0.88) or by Multi-layer Insulation (MLI, solar albedo 0.95, IR emissivity 0.05). For the sake of simplicity we assume, for now, that the lander has a constant temperature of 250 K. With regard to the material properties of the ground we adopt the values of the Oxford Thermal Model [1], except for the solar albedo, which we assume to be constant at 0.12. Regarding scattered light we currently consider only single-scattering. First the surface temperature of the undisturbed plane is determined for epoch 2025-03-07T12:00:00 UTC. On this date the lander is placed on the surface. For all subsequent times the ground temperature is computed taking the lander's presence into account.

Results: Figures 1-4 show temperature curves for a location about 33 cm in front of the lander, where the corresponding lander side is directed to the North. The black curve shows the temperature without the lander, the orange curve shows the temperature when single-scattering and the red curve when single-scattering and thermal emission from the lander are taken into account. Figure 1 compares the temperature curves during one month for a lander whose surface consists of black paint. Due to the low albedo, single scattering only increases the temperature of the ground by a maximum of 7K. The thermal emissions from the lander, on the other hand, increase the temperature of the ground by up to 25 K. At the same time, the ground does not cool down as much during the night as it would without the lander's presence. Figure 2 provides a closer look at the first two hours after landing and demonstrates that the ground responds quickly to the

lander's presence.

Figure 3 shows the temperature curves over the course of one month for a lander whose surface consists of MLI. Due to the lander's large albedo, single scattering increases the temperature of the ground by up to 90 K. However, due to the lander's small emissivity, thermal emissions from the lander are negligible during the daytime. At night, they prevent the ground from cooling down as much as it would without the lander. Again, Figure 4 shows the first two hours after landing in more detail.

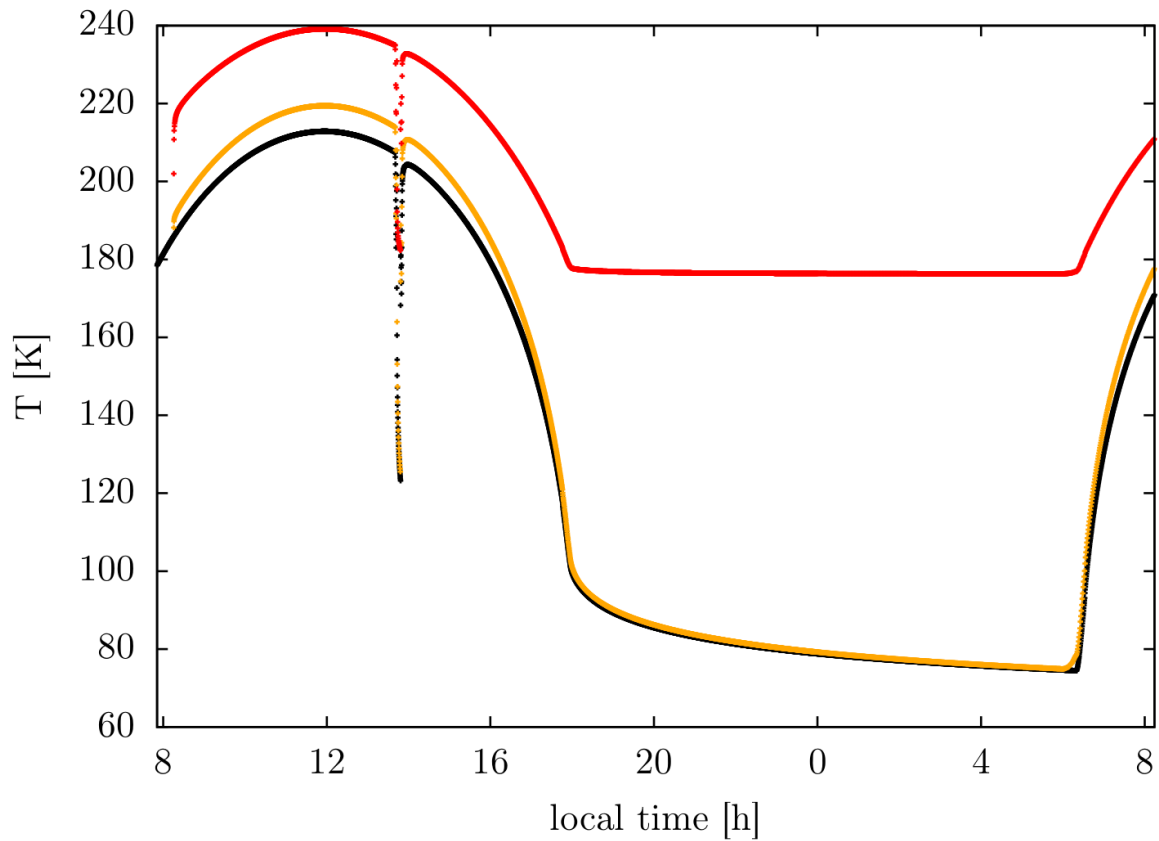


Figure 1: The temperature at the North side of the lander at a distance of 33 cm for a lander covered with black paint. Black: Temperature without the lander's presence. Yellow: Single-scattering included. Red curve: Single-scattering and thermal emissions included. Before the arrival of the lander at around 8:25 am local time, the three curves are identical. Around 2 pm an eclipse occurs.

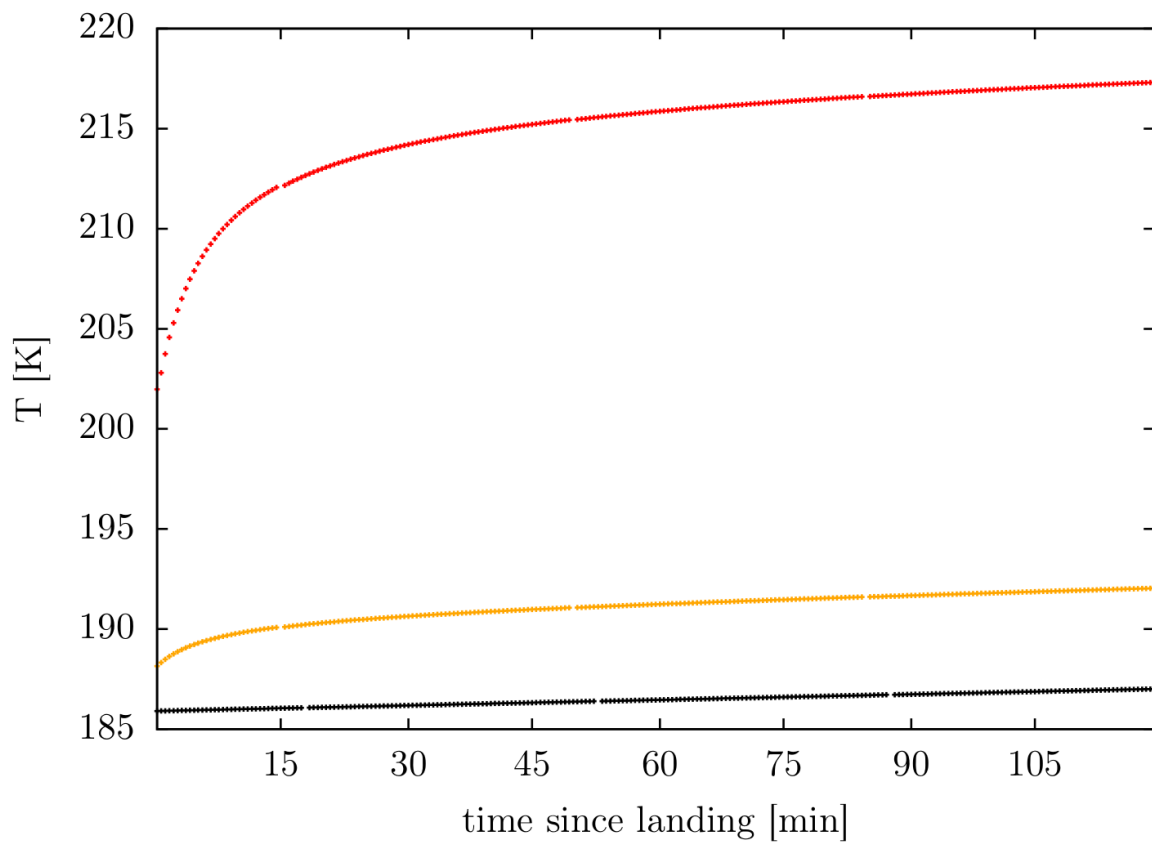


Figure 2: The temperature at the North side of the lander at a distance of 33 cm for the first two hours after the landing. For an explanation of the color code see Figure 1.

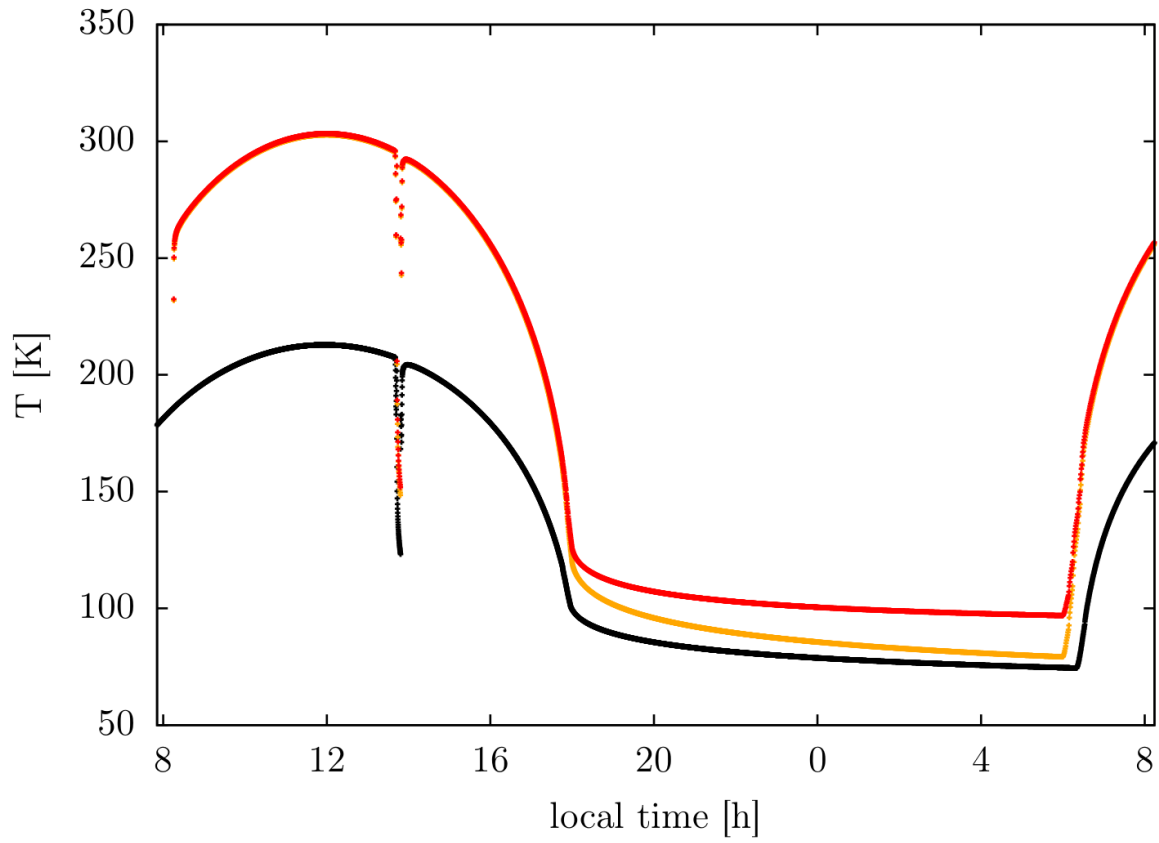


Figure 3: The temperature at the North side of the lander at a distance of 33 cm for a lander covered with MLI. For an explanation of the color code see Figure 1. Before the arrival of the lander at around 8:25 am local time, the three curves are identical. During daytime the orange and the red curve are identical, too. Around 2 pm an eclipse occurs.

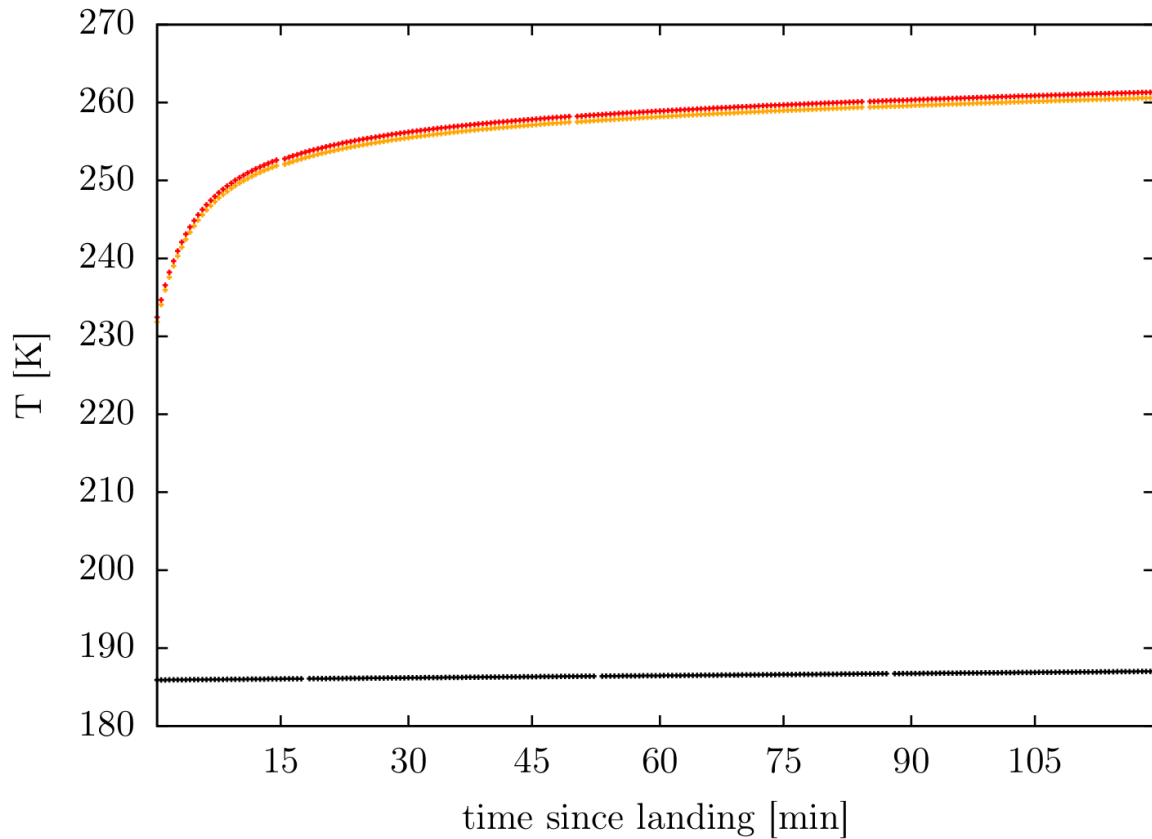


Figure 4: The temperature at the North side of the lander at a distance of 33 cm for the first two hours after the landing. For an explanation of the color code see Figure 1.

Summary and Outlook: If the temperature of the regolith is measured, the presence of the lander must be taken into account, especially if conclusions are to be drawn about the material properties from the temperature.

The next steps are to increase the resolution of the meshes and run our code in multi-scattering mode. Moreover, the lander's temperature will be calculated more accurately. We also plan to study a landing site at the Shackleton - de Gerlache ridge and the case of a lander situated inside a permanently shadowed region.

Acknowledgements: LRAD is supported by the German Federal Ministry for Economic Affairs and Climate Action on the basis of a decision by the German Bundestag. Grant: 500W2103

References: [1] King et al. (2020), PSS 182. doi:10.1016/j.pss.2019.104790